Effect of electron beam irradiation on filtering facepiece respirators integrity and filtering efficiency

Dagmara Chmielewska-Śmietanko[1], Łukasz Werner[2], Urszula Gryczka[1], and Wojciech Migdał[1]

[1]Institute of Nuclear Chemistry and Technology
[2]Warsaw University of Technology

July 25, 2020

Abstract

The outbreak of the COVID-19 pandemic has showed that the need for medical masks and respirators exceeds the current global stockpile of these item and production capacity. Taking into account that ionizing radiation has been used for sterilization of medical products for many years and electron beam irradiation enables the treatment of huge quantities of disposable medical products in a short time this method should be tested for the masks decontamination. In this work two different filtering facepiece respirators were irradiated with electron beam of different doses. Presented results confirmed that the decrease in filtration efficiency after irradiation of both respirators results from elimination of the electric charge from the PP fibers in the irradiation process. Nevertheless, applied doses did not influence filtering materials structure and integrity, therefore application of treated in this way masks can be considered after restoration of electric charge what is crucial for their filtering function.

1. Introduction

The discussion around transmission routes of the SARS-CoV-2 virus has been accompanying the outbreak of the COVID-19 pandemic. Currently available research supports the theory that the virus could be spread not only by direct contact with the infected person, contaminated surfaces or fomites but may also be spread by airborne transmission [1-3]. Respiratory droplets that may contain virus particles could be generated not only during the coughing or sneezing but also are produced during laughing, breathing or speaking [4]. Moreover, size of the expiratory particles emitted in each of these activities is different [4].

Larger droplets precipitate quickly in the ground or another surface before drying, but smaller ones may stay long in the air become aerosolized particles.

Therefore, special safety measures like hand-washing, social distance and use of personal protective equipment (PPE) like filtering facepiece respirators should be implemented to prevent the SARS-CoV-2 transmission.

Generally, most PPE is designed to be used only one time and by one person prior to disposal, should not be reprocessed and reused. Exposition of PPE to infectious materials during use (e.g., body fluids from an infected person) results its microbiological contamination therefore used PPE should be removed promptly, using proper removal and disposal procedures.

However, the outbreak of the COVID-19 pandemic has showed clearly that the current global stockpile of PPE is insufficient, particularly for medical masks and respirators (FFP3 or FFP2 standard). Moreover, the capacity to expand PPE production is limited therefore, the current demand for respirators and masks cannot be met and the shortages of PPE has become a global problem. This issue has led to serious consideration of temporary measures that can be adopted in crisis situations when serious shortage of PPE takes place. Based on current evidence, in consultation with international experts WHO carefully considered possibility of the reprocessing and reuse of the PPE [5]. The FDA also has issued Emergency Use Authorizations (EUAs) for the emergency use of decontamination systems for certain respirators used by health care personnel when there are insufficient supplies of new respirators resulting from the COVID-19 pandemic. However, reprocessing should not affect integrity of the filtration materials and respirators after decontamination should still fulfil strict requirements concerning filtration effectiveness. Different methods as hydrogen peroxide sterilization, ethylene oxide fumigation, UV, microwave oven irradiation or hot water heating were tested for decontamination of filtering facepiece respirators [6-9].

Ionizing radiation has been widely used for sterilization of disposable medical products for many years [10]. Different types of ionizing radiation, i.e., γ- radiation from isotopic sources, high-energy X-rays from high-power X-ray generators or electron beams (EB) from accelerators can be applied to radiation sterilization of medical disposable products.

EB irradiation enables the treatment of huge quantities of disposable medical products in a short time. However, electron beam is characterized with lower penetration than γ-rays, therefore, products of higher density should be properly packed to be successfully sterilized. Nevertheless, due to high dose rate of EB irradiation the decontamination of PPE is very fast process and appropriate dose is delivered in several seconds what could limit post-oxidation related effects related to degradation of the materials (polymers) that were used to PPE production [11].

It was confirmed that ionizing radiation is very effective in coronaviruses elimination and doses D_{10} do not exceed 2 kGy [12, 13]. The D_{10} value is the dose required to reduce an exposed microbial population 90% (one $\log_{10}$) at a given conditions.

In this work two different filtering facepiece respirators (one conforming to the FFP1 standard and one conforming to the FFP3 standard) were irradiated with electron beam of different doses. Then effect of EB irradiation on filtration efficiency, morphology and degradation of the masks material was evaluated.

2. Materials and methods

To compare influence of EB irradiation on different respirators two different polypropylene masks: 3M 1863+ conforming to the high FFP3 standard and 3M 9101E conforming to the FFP1 standard were chosen for the investigation. Masks were sealed in plastic bags and irradiated with doses 12 kGy and 25 kGy in air atmosphere, at ambient temperature. Electron beam irradiation of samples was carried out using 10 MeV, 10 kW linear electron accelerator "Elektronika". Delivered doses were confirmed using B3 radiochromic foil dosimeter measured with a flat bed scanner and RisoScan software, with uncertainties evaluated at 8%. The masks were irradiated in a single layer to minimise dose gradient and ensure uniformity of delivered doses. For both tested samples the dose increase inside the samples was below 1 %.

Doses were selected taking into account assumption the possible variability in viral load in used masks and its random distribution among products. On the base of microbial contamination found in surgical masks one can realise that the standard deviation of the bioburden is higher than the mean N: 47 ± 56 cfu/ml/piece for inside mask area and 166 ± 199 cfu/ml/piece from mask outside area [14]. This results from the variability of environments where masks are used and differences in the level of the bioburden. On the base of the maximum of 1000 microorganisms should be present in the product, decontamination dose (a dose required for 5 or 6 order of magnitude reduction of bioburden) was calculated as 12 kGy [14]. Moreover, masks were also irradiated with standard sterilization dose 25 kGy which is defined as sterilization dose according to VD_{max} method given in ISO 11137-2 standard "Sterilization of health care products — Radiation — Part 2: Establishing the sterilization dose".. Masks that were not irradiated were used as control samples.

SEM images of the masks layers were obtained, using a Hitachi TM-100 scanning electron microscope with an accelerating voltage of 15.0kV. Samples for the SEM examination were prepared according to a standard procedure, fixed with conductive glue, and coated with a thin layer of gold. The samples were examined at a magnification of 500×.

Thermogravimetric analysis (TGA) of masks samples was used to determine the thermal stability and possible degradation of respirators materials was conducted with a Q500 TGA (TA Instruments) thermogravimetric analyser in the temperature range 37–700°C at a heat ingrate of 10°C per minute, under a constant flow (60 mL/min) of nitrogen gas.

To determine the initial separation efficiency of the tested respirators samples before and after irradiation the high quality test bench MFP NanoPlus (PALAS GmbH) was used. The main elements of this test-rig are: UGF2000 generator which is able to generated nanoobject from liquid solution, cascade of impactors which were used to cut-off the largest particles (which were not object of this research), the bipolar neutralizer Kr-85, used to ensure equilibrium charge distribution on particles, DEMC classification column, pneumatic filtration chamber and universal fluid condensation particle counter UF-CPC. The UF-CPC together with the DEMC classification column form a system called U-SMPS. It allows to classify and count particles in size range from 20 to 200 nm. Scheme of MFP nanoPlus is presented in Fig.1.

Fractional and overall filtration effectiveness was determined for solid particles (KCl nanocrystals) as well as oil nanodroplets of Di-Ethyl-Hexyl-Sebacat (DEHS). For tests circular samples with diameter of 60 mm were punched from tested respirators. All filtration test were performed at the air flow rate 95 L/min and the air face velocity 0.559 m/s. For this experiments It was required to performed experiments in a sequence of measurements without (upstream) and with (downstream) a filtrating material in the tested chamber. One series consisted of two upstream measurements and two downstream measurements. There were carried out two series of measurements for each masks material. Next, the average value of the filtration effectiveness was calculated and presented on diagrams below. The time of a single measurement of upstream and downstream was always 380 sec. For this time, the interval between measurements was included and it was 60 sec. Such a long time of a single measurement was necessary to correctly classify and count nanoparticles. Moreover, during the tests there were also determined the pressure drops across the tested materials and their initial overall filtration efficiency. Size distribution of the generated aerosols used in the experiments is presented in Fig. 2.

Results and discussion

SEM images of the separate layers that compose 1863+ and 9101E respirators are presented in Fig. 3 and Fig. 4, respectively.

Filtration material used in both tested respirators was composed of pure polypropylene (PP), however investigation of the 1863+ respirator filtration fabric revealed that the mask consist of four layers, each of them is composed of the PP fibres of different diameters woven in different density (Fig. 3). Filtration media that composes 9101E respirator consists of three layers, inner and outer fabric seems to be built of the fibres of similar diameter and density, while middle layer is composed of the fibres of significantly smaller diameters (Fig. 4).

Any holes or cracks in the fibres structure are not visible therefore one can conclude that applied irradiation doses do not effect morphology of the fibres used for the respirators production.

The investigation of the thermal properties of respirators irradiated with different EB doses was carried out in order to determine influence of radiation on thermal stability. Filtration materials can undergo degradation or cross-linking under irradiation. In case of the 1863+ respirator small degradation of the material was confirmed. The higher irradiation dose was the higher drop of onset temperature and temperature of the maximum in the loss weight rate was observed (Fig. 5 and Fig. 6). However, observed decrease of the characteristic temperatures is not big therefore degradation of the filtration material under EB irradiation is minimal. Thermal decomposition of the material is single step process with one peak in temperature ˜445-460 °C which is characteristic for PP degradation (Fig. 6).

Completely deferent phenomena in the thermal degradation of the 9101E filtration material is observed. Onset temperature determined for the filtration materials increase with irradiation dose (Fig. 7). Thermograms obtained for control sample and the sample irradiated with 12 kGy are characteristics for non-oxidized PP, while peak present in the thermogram of the sample irradiated with 25 kGy is typical for oxidized PP (Fig. 8) [15]. Therefore, one can conclude that oxidation of the PP took place in the irradiation process and the higher dose was applied the level of PP oxidation was higher. PP oxidation lead to increase of the material thermal stability and can be connected with reduction of the third type hydrogen and formation of carboxylate salt (COO-N-Me3Ph) in oxidized PP [16].

It was observed decrease in filtration efficiency for irradiated respirators in comparison to the control samples. Decrease in filtration efficiency observed for respirators irradiated with both doses was similar. Moreover, for both respirators it was observed that filtration efficiency decreased with the increase of the particle diameter (Fig. 9). The main mechanical mechanism of deposition for nanoparticles is diffusion (Brownian motion). When the particle diameter increases, the Brownian motion are less intense, thus and diffusional mechanism becomes less important in process of particle deposition, which explain the observed phenomenon.

Decrease in filtration efficiency may result from elimination of the electric charge from the PP fibers in the irradiation process. To support this theory conditioning of the non-irradiated samples of respirators in isopropanol (IPA) vapours was applied to remove the electric charge from the surface of studied filtrating materials. Obtained results confirmed that drop in filtration efficiency for the irradiated filters is connected with the elimination of the electric charge from the fiber surface (Fig. 10).

Baseline filtration efficiency was very high for both respirators: 99.7% for 1863+ respirator and 90.2% for 9101E respirator, whereas after irradiation with both doses filtration efficiency dropped to 62% (average value for droplets and particles filtration) for respirator 1863+ irradiated with 12 kGy and similar value 66% was obtained for this respirator irradiated with 25 kGy. Even more significant decrease in filtration efficiency to 42% for respirators irradiated with 12 kGy and 44% for masks irradiated with 25 kGy was observed for 9101E respirator (Fig. 11). The decrease of filtration efficiency observed for control samples conditioned in IPA was similar to the drop in filtration efficiency determined for irradiated samples what supports theory that irradiation eliminate electric charge from the surface of PP fibres. Moreover, filtration efficiency observed for irradiated samples conditioned additionally in IPA remained almost at the same level.

Additionally, pressure drop across the filtrating materials was determined for each respirators do investigate influence of the irradiation on the integrity and stability of the filtration materials (Fig. 13). Small decrease of the pressure drop across the filtrating materials after irradiation was observed for both respirators. However, observed differences in pressure drop for control and irradiated samples were so small that can not be connected with the changes of the filtrating materials structure.

Conclusions

Irradiation of two different filtering facepiece respirators with electron beam irradiation allows to determine that applied irradiation doses does not affect filtrating materials stability and integrity. SEM analysis revealed that morphology of the fibres used for the respirators production remains the same after irradiation with both doses as the morphology of control samples and any effect like crack and holes are not visible for all filtrating layers . In case of the 1863+ respirator slight degradation of the material was confirmed while completely different behaviour was observed for 9101E respirator.

Presented results confirmed that the decrease in filtration efficiency after irradiation of both respirators results from elimination of the electric charge from the PP fibers in the irradiation process. Therefore, decontamination of filtering facepiece respirators with electron beam irradiation is problematic without regard to applied doses. Nevertheless, applied doses did not influence filtering materials structure and integrity, therefore application of treated in this way masks can be considered after restoration of electric charge what is crucial for their filtering function.

Acknowledgement

Hosted file

`image1.emf` available at https://authorea.com/users/345974/articles/472046-effect-of-electron-beam-irradiation-on-filtering-facepiece-respirators-integrity-and-filtering-efficiency

This project has received funding from the European Union's Horizon 2020 Research and Innovation programme under grant agreement No 730871.

This work was supported by the Polish Ministry of Science and Higher Education, project 3697/H2020/2017/2 Accelerator Research and Innovation for European Science and Society.

References

[1] Yu L T, Li Y, Wong T W, Tam W, Chan A T, Lee J H, Leung D Y, Ho T. Evidence of airborne transmission of the severe acute respiratory syndrome virus. N. Engl. J. Med. 2004; 350:1731-1739.

[2] van Doremalen N, Bushmaker T, Morris D H, Holbrook M G, Gamble A, Williamson B N, Tamin A, Harcourt J L, Thornburg N J, Gerber S I, Lloyd-Smith J O, de Wit E, Munster V J. Aerosol and Surface Stability of SARS-CoV-2 as Compared with SARS-CoV-1, N. Engl. J. Med. 2020;382:1564-1567.

[3] Morawska L, Cao J. Airborne transmission of SARS-CoV-2: The world should face the reality. Environ Int. 2020;139:105730.

[4] Morawska L, Johnson G R, Ristovski Z D, Hargreaves M, Mengersen K, Corbett S, Chao C Y H, Li Y, Katoshevski D. Size distribution and sites of origin of droplets expelled from the human respiratory tract during expiratory activities. J. Aerosol Sci. 2009;40:256-269.

[5] Rational use of personal protective equipment for coronavirus disease (COVID-19) and considerations during severe shortages. Interim guidance., World Health Organization, Geneva, 6 April 2020.

[6] Viscusi D J, Bergman M S, Eimer B C, Shaffer R E. Evaluation of five decontamination methods for filtering facepiece respirators. Ann. Occup. Hyg. 2009;53:815-827.

[7] Mackenzie D. Reuse of N95 Masks. Engineering. 2020; 6:593-596.

[8] Schwartz M S A, Greeson N, Vogel A, Thomann W, Brown M, Sempowski G D, Alderman T S, Condreay J P, Burch J, Wolfe C, Smith B, Lewis S. Decontamination and Reuse of N95 Respirators with Hydrogen Peroxide Vapor to Address Worldwide Personal Protective Equipment Shortages During the SARS-CoV-2 (COVID-19) Pandemic. Appl Biosaf. 2020;25:67-70.

[9] Lindsley W G, Martin S B, Thewlis R E, Sarkisian K, Nwoko J O, Mead K R, Noti J D. Effects of Ultraviolet Germicidal Irradiation (UVGI) on N95 Respirator Filtration Performance and Structural Integrity. J. Occup. Environ. Hyg. 2015;12:509-517.

[10] Chmielewski A G. Practical Applications of Radiation Chemistry. Russ. J. Phys. Chem. A. 20007;81:1488-1492.

[11] Chmielewska-Śmietanko D, Gryczka U, Migdał W, Kopeć K. Electron beam for preservation of biodeteriorated cultural heritage paper-based objects, Radiat. Phys. Chem. 2018;143:89-93.

[12] Gamma irradiation as a treatment to address pathogens of animal biosecurity concern Final policy review in: Department of Agriculture (Ed.)Canberra, November 2014.

[13] Feldmann F, Shupert W L, Haddock E, Twardoski B, Feldmann H. Gamma Irradiation as an Effective Method for Inactivation of Emerging Viral Pathogens. Am. J. Trop. Med. Hyg. 2019;100:1275-1277.

[14] Sterilization and reprocessing of personal protective equipment (PPE), including respiratory masks, by ionizing radiation IAEA Technical Report, International Atomic Energy Agency, Vienna, 2020.

[15] Reisi Nafchi H, Abdouss M, Kazemi Najafi S, Mohebbi Gargari R, Mazhar M. Effects of nano-clay particles and oxidized polypropylene polymers on improvement of the practical properties of wood-polypropylene composite. Adv. Compos. Mater. 2015;24:239-248.

[16] Abdouss M, Sharifi-Sanjani N, Bataille P. Oxidation of polypropylene in a solution of monochlorobenzene. J. Appl. Polym. Sci.1999;74:3417-3424.

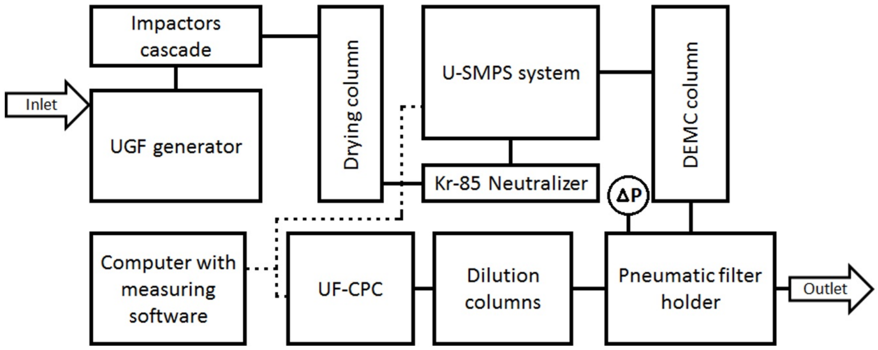

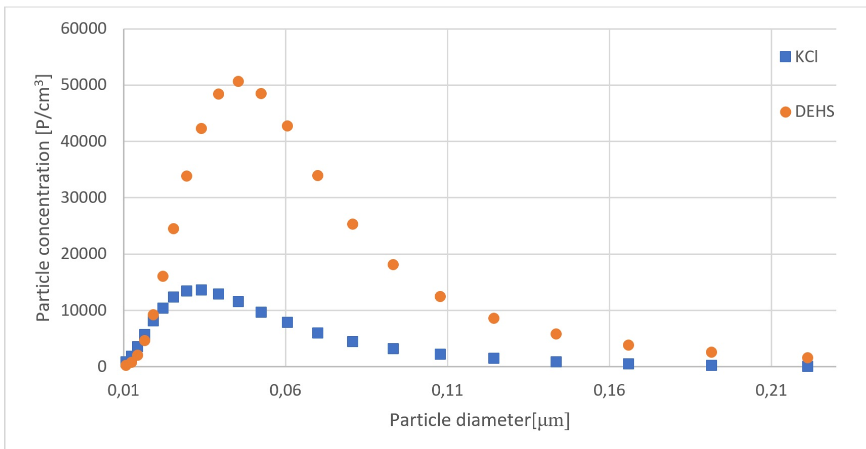

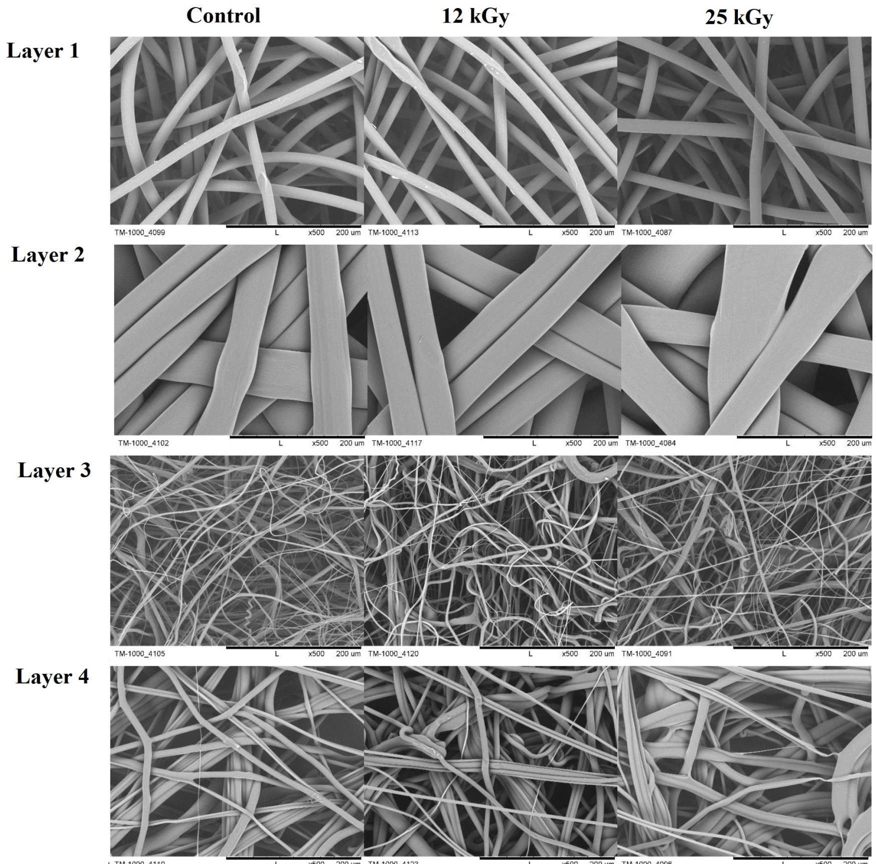
Control
12 kGy
25 kGy
Layer 1
Layer 2
Layer 3
Layer 4

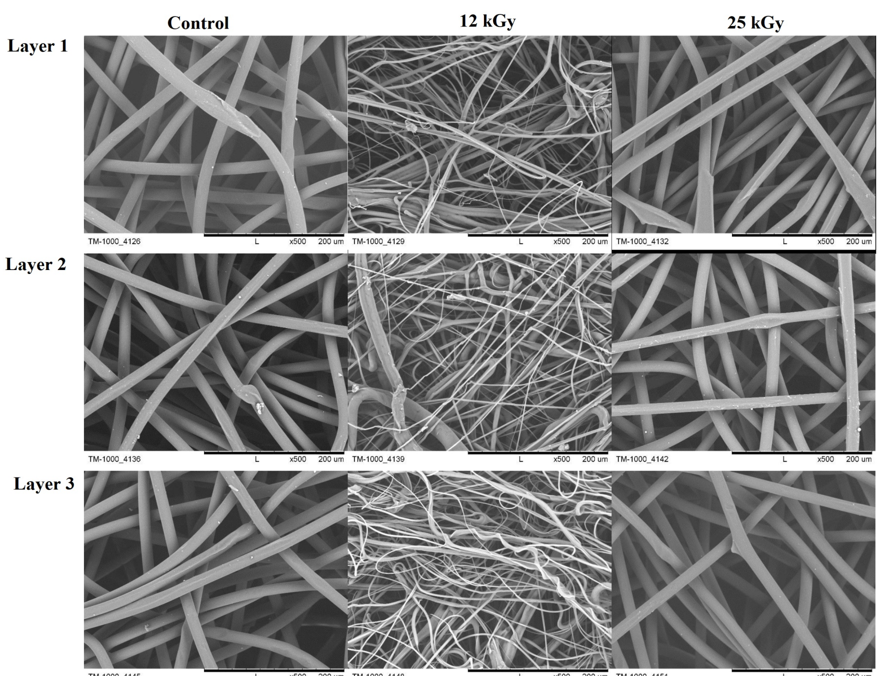
Control
12 kGy
25 kGy
Layer 1
Layer 2
Layer 3

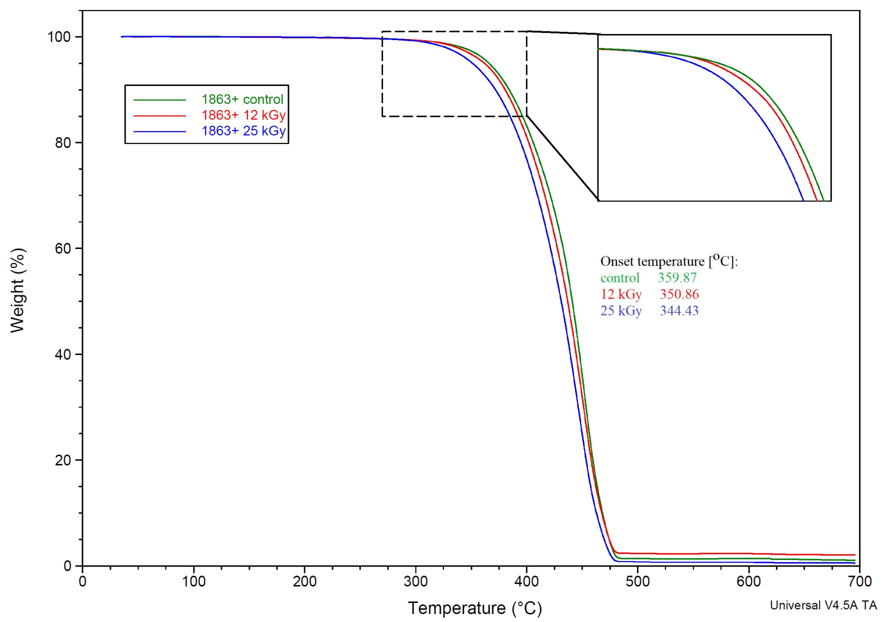
1863+ control
1863+ 12 kGy
1863+ 25 kGy
Onset temperature [°C]:
control 359.87
12 kGy 350.86
25 kGy 344.43
Weight (%)
Temperature (°C)
Universal V4.5A TA

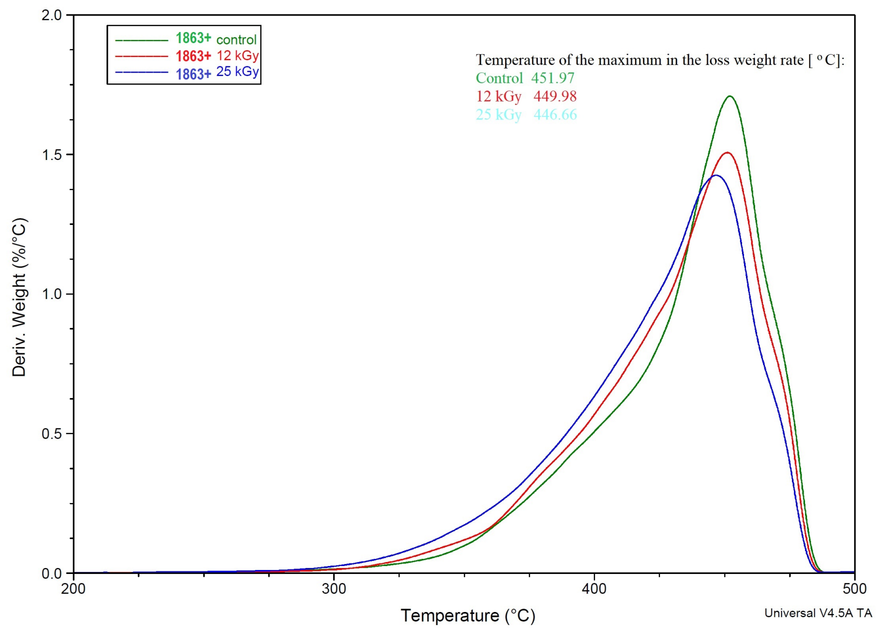
1863+ control
1863+ 12 kGy
1863+ 25 kGy
Temperature of the maximum in the loss weight rate [°C]:
Control 451.97
12 kGy 449.98
25 kGy 446.66
Deriv. Weight (%/°C)
Temperature (°C)
Universal V4.5A TA

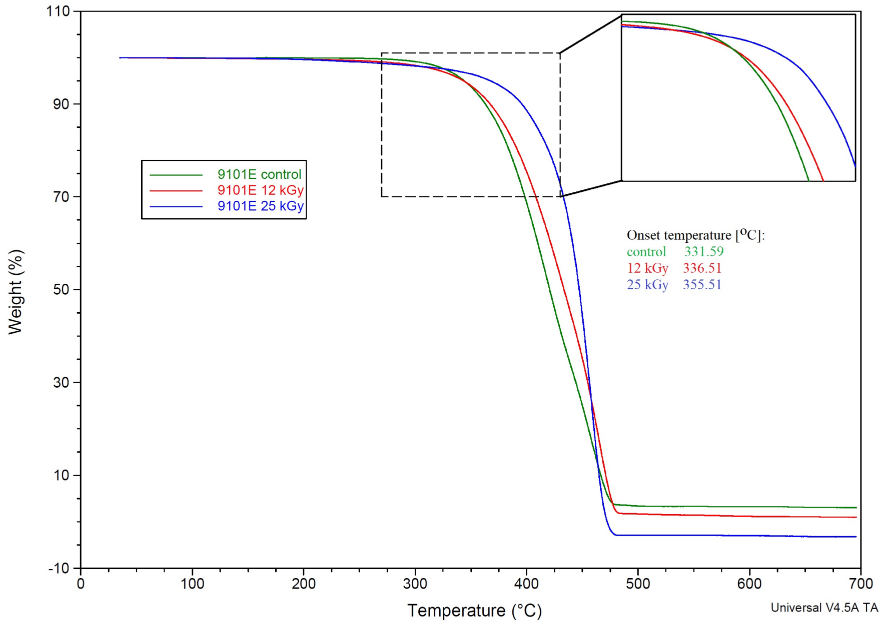
110
90
70
50
30
10
-10
Weight (%)
0
100
200
300
400
500
600
700
Temperature (°C)
Universal V4.5A TA
9101E control
9101E 12 kGy
9101E 25 kGy
Onset temperature [°C]:
control 331.59
12 kGy 336.51
25 kGy 355.51

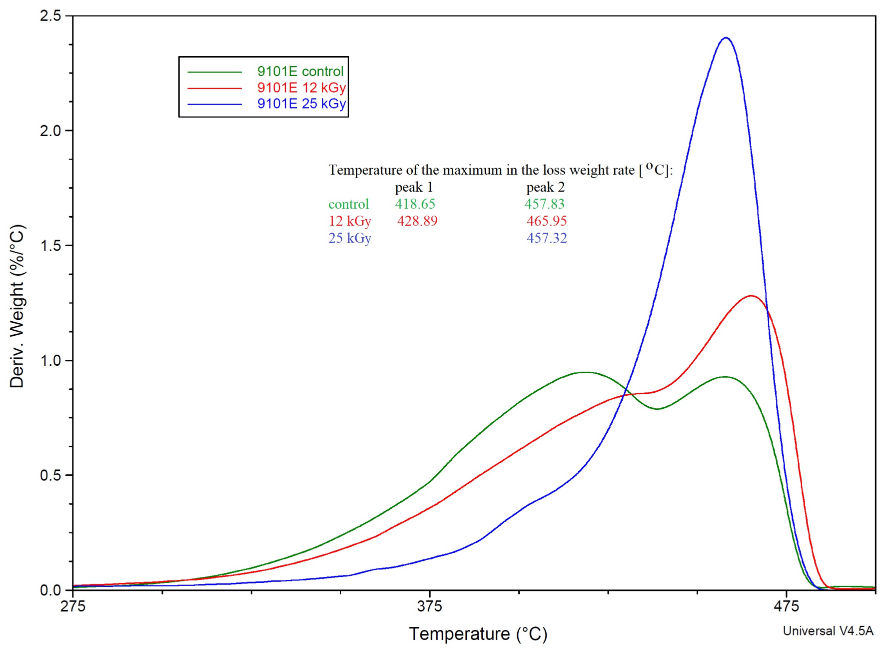
2.5
2.0
1.5
1.0
0.5
0.0
Deriv. Weight (%/°C)
275
375
475
Temperature (°C)
Universal V4.5A
9101E control
9101E 12 kGy
9101E 25 kGy
Temperature of the maximum in the loss weight rate [°C]:
peak 1
peak 2
control 418.65 457.83
12 kGy 428.89 465.95
25 kGy 457.32

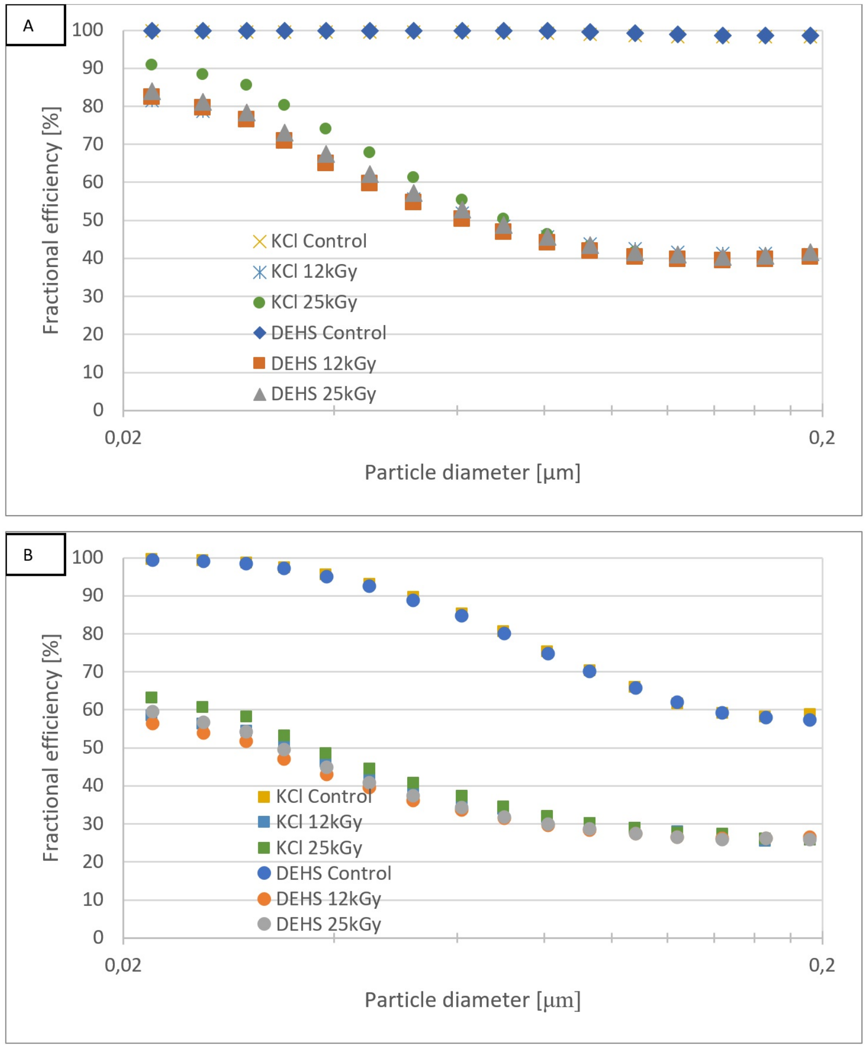
A
Fractional efficiency [%]
100
90
80
70
60
50
40
30
20
10
0
0,02
0,2
Particle diameter [µm]
KCl Control
KCl 12kGy
KCl 25kGy
DEHS Control
DEHS 12kGy
DEHS 25kGy
B
Fractional efficiency [%]
100
90
80
70
60
50
40
30
20
10
0
0,02
0,2
Particle diameter [µm]
KCl Control
KCl 12kGy
KCl 25kGy
DEHS Control
DEHS 12kGy
DEHS 25kGy

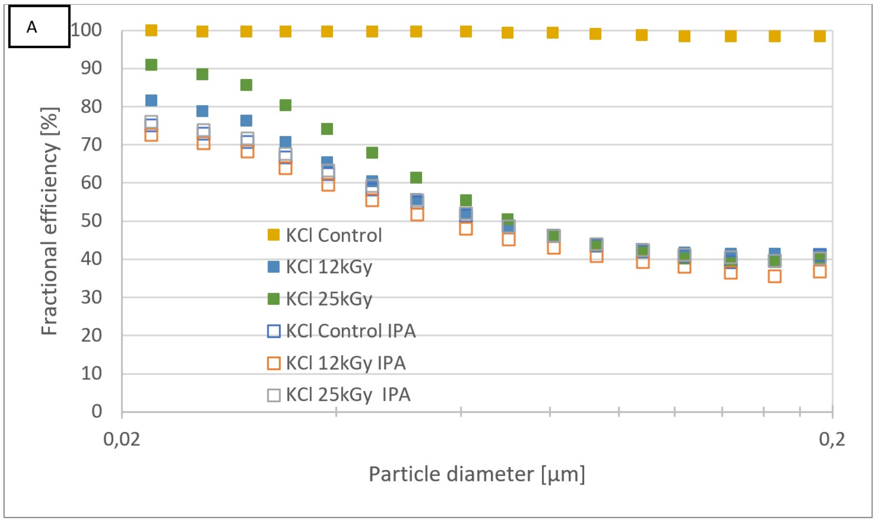
A
Fractional efficiency [%]
100
90
80
70
60
50
40
30
20
10
0
0,02
0,2
Particle diameter [µm]
KCl Control
KCl 12kGy
KCl 25kGy
KCl Control IPA
KCl 12kGy IPA
KCl 25kGy IPA

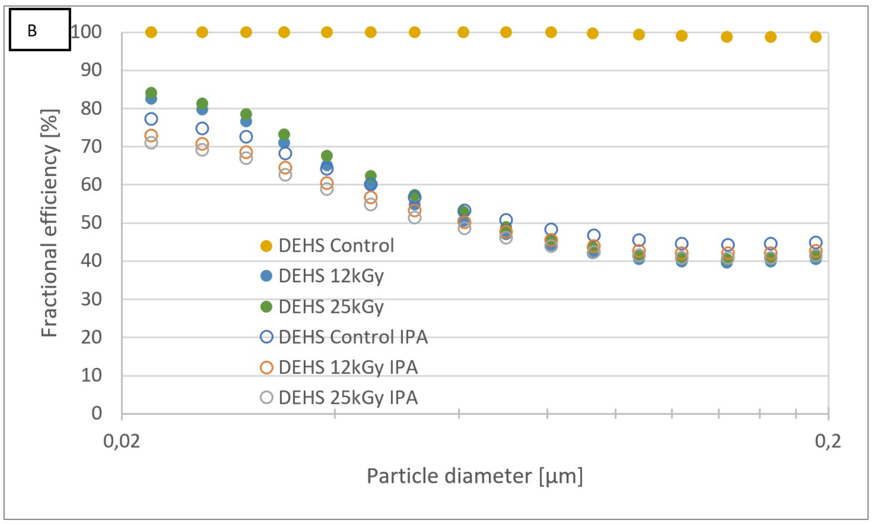
B
Fractional efficiency [%]
100
90
80
70
60
50
40
30
20
10
0
0,02
0,2
Particle diameter [µm]
DEHS Control
DEHS 12kGy
DEHS 25kGy
DEHS Control IPA
DEHS 12kGy IPA
DEHS 25kGy IPA

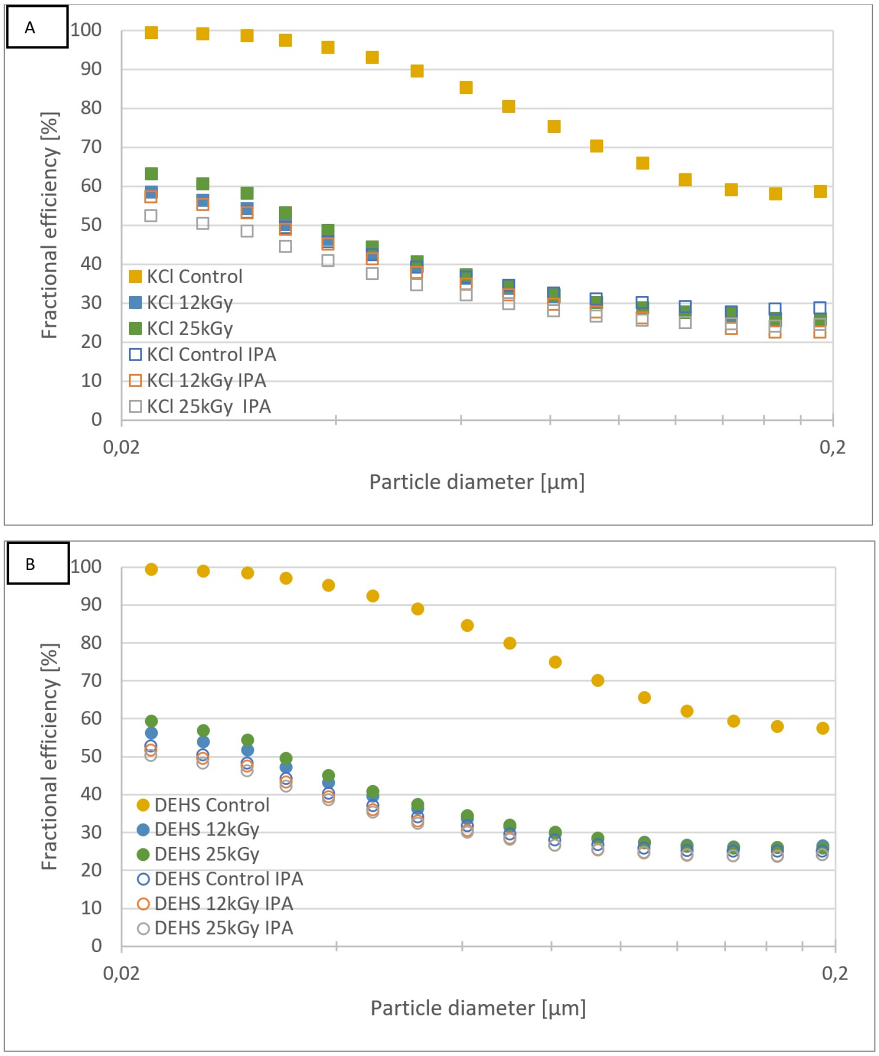
A
Fractional efficiency [%]
0
10
20
30
40
50
60
70
80
90
100
KCl Control
KCl 12kGy
KCl 25kGy
KCl Control IPA
KCl 12kGy IPA
KCl 25kGy IPA
0,02
0,2
Particle diameter [µm]
B
Fractional efficiency [%]
0
10
20
30
40
50
60
70
80
90
100
DEHS Control
DEHS 12kGy
DEHS 25kGy
DEHS Control IPA
DEHS 12kGy IPA
DEHS 25kGy IPA
0,02
0,2
Particle diameter [µm]

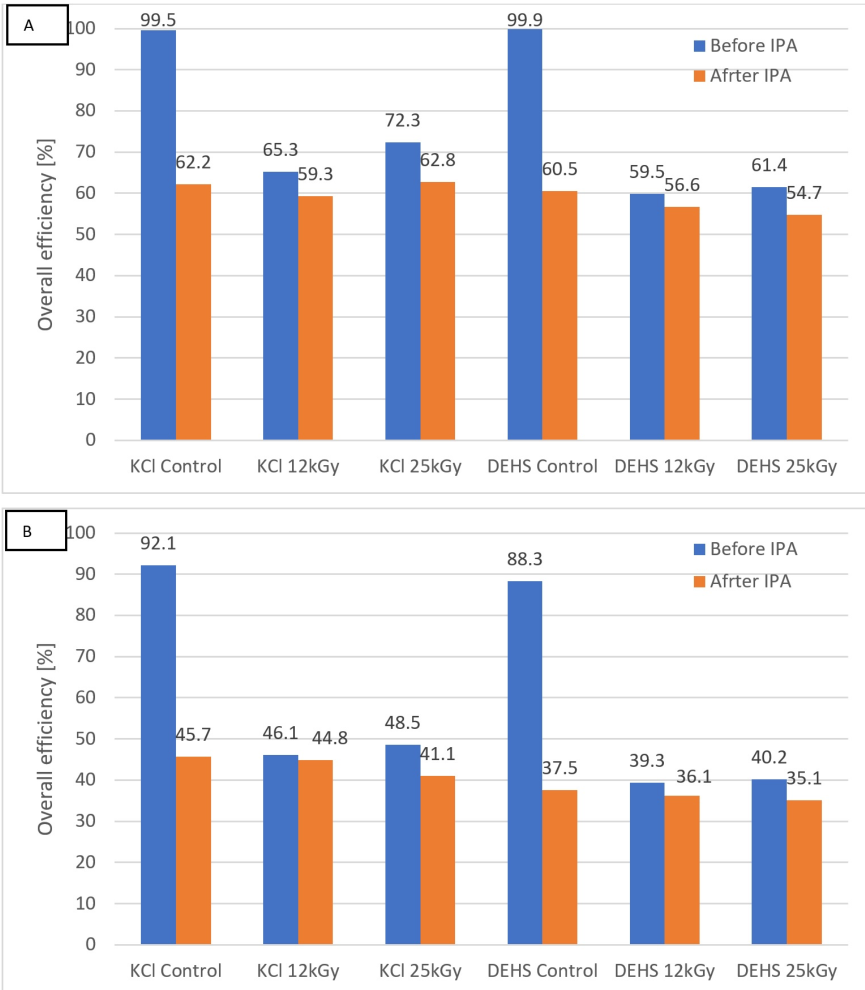
A
Overall efficiency [%]
100
90
80
70
60
50
40
30
20
10
0
99.5
62.2
65.3
59.3
72.3
62.8
99.9
60.5
59.5
56.6
61.4
54.7
Before IPA
Afrter IPA
KCl Control
KCl 12kGy
KCl 25kGy
DEHS Control
DEHS 12kGy
DEHS 25kGy
B
Overall efficiency [%]
92.1
45.7
46.1
44.8
48.5
41.1
88.3
37.5
39.3
36.1
40.2
35.1
Before IPA
Afrter IPA
KCl Control
KCl 12kGy
KCl 25kGy
DEHS Control
DEHS 12kGy
DEHS 25kGy

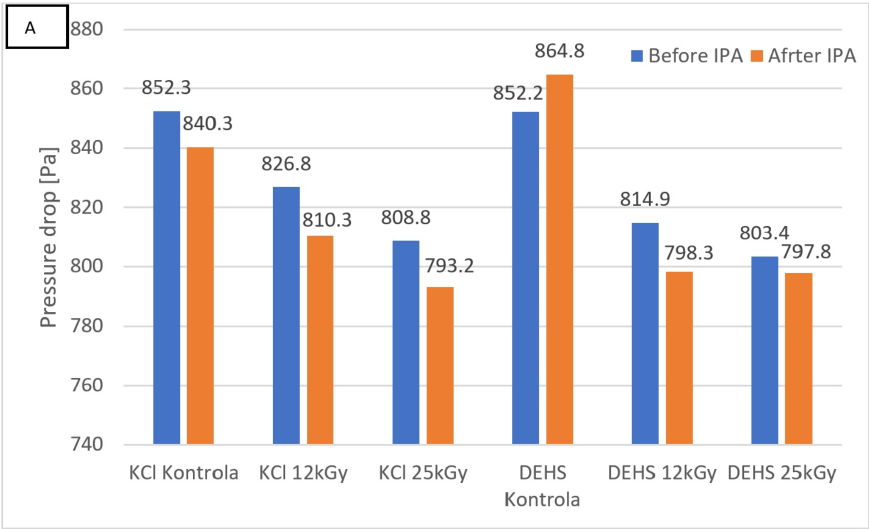
A
Pressure drop [Pa]
880
860
840
820
800
780
760
740
Before IPA
Afrter IPA
852.3
840.3
826.8
810.3
808.8
793.2
852.2
864.8
814.9
798.3
803.4
797.8
KCl Kontrola
KCl 12kGy
KCl 25kGy
DEHS Kontrola
DEHS 12kGy
DEHS 25kGy

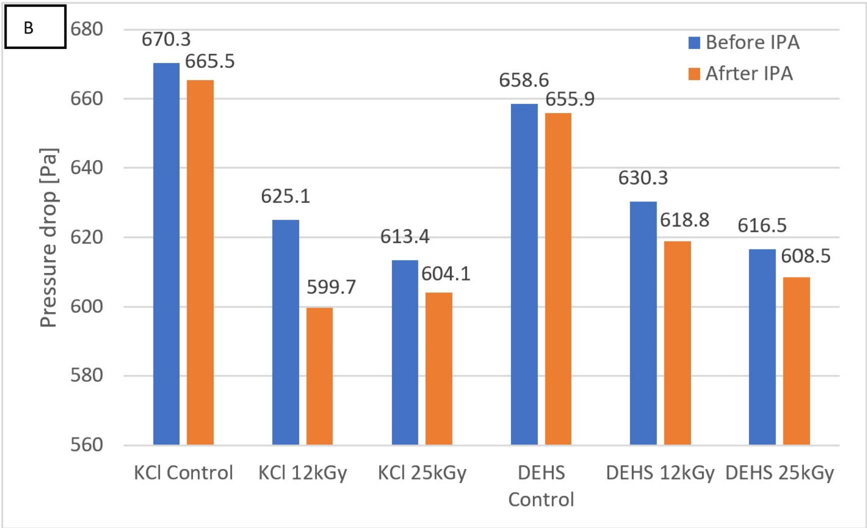
B
Pressure drop [Pa]
680
660
640
620
600
580
560
Before IPA
Afrter IPA
670.3
665.5
625.1
599.7
613.4
604.1
658.6
655.9
630.3
618.8
616.5
608.5
KCl Control
KCl 12kGy
KCl 25kGy
DEHS Control
DEHS 12kGy
DEHS 25kGy